Chemical Engineering Science, 1973, Vol. 28, pp. 1169–1177. Pergamon Press. Printed in Great Britain

A structural model for gas–solid reactions with a moving boundary—IV. Langmuir–Hinshelwood kinetics

H. Y. SOHN and J. SZEKELY
Department of Chemical Engineering and Center for Process Metallurgy, State University of New York at Buffalo, Buffalo, New York 14214, U.S.A.

(*Received* 28 *June* 1972; *accepted* 6 *October* 1972)

Abstract—The Langmiur–Hinshelwood type of kinetic expression has been incorporated into the "general structural model" for the reaction of a porous solid with a gas. Thus the system occupies the domain between the asymptotes corresponding to first-order and zeroth-order kinetics.

The effect of the form of the rate expression is found to be the largest in the intermediate regime where both chemical reaction and diffusion play important roles in determining the overall rate. A "gas–solid reaction modulus" generalized for the Langmuir–Hinshelwood type of rate expression was developed to define the regimes of the different controlling mechanisms.

INTRODUCTION

IN A PREVIOUS paper we developed a generalized model for the reaction between a porous solid and a reactant gas, for systems with first-order kinetics with respect to the reactant gas [1]. The model provided general criteria for relating structural effects to the reactivity of porous solids and the reaction modulus defined therein allowed the assessment of the relative importance of pore diffusion and chemical kinetics.

While almost all the mathematical models for gas–solid reaction systems are based on the assumption of first-order kinetics, there is reason to believe that in many instances the Langmuir–Hinshelwood type rate expression provides a more realistic description of the system, especially over a wide range of reactant concentration. Examples of gas–solid reactions that have been found to follow a Langmuir–Hinshelwood type kinetics include the reduction of iron oxides by hydrogen [2, 3], the reduction of nickel by hydrogen [4], the oxidation of uranium–carbon alloys [5], and the reaction of carbon with various gases [6]. Further examples can be found in the literature [e.g. 7].

The purpose of the work described in this paper is to develop a generalization of the structural model presented in Ref. [1], by incorporating Langmuir–Hinshelwood type kinetics in the reaction scheme. The principal motivation for the work has been to provide means for the interpretation of experimental data in terms of a structural model and to define the regions of validity for the assumption of first-order kinetics.

While the use of non-linear kinetics in gas–solid reactions (involving porous solids) is a rather unexplored field, a great deal of work has been done on the effect of Langmuir–Hinshelwood type kinetics on the effectiveness factor in heterogeneous catalysis [8–11].

Let us consider the following rate expression for the surface reaction:

$$R_A = \frac{kP_A}{1+KP_A} \tag{1}$$

where R is the local reaction rate; P_A is the partial pressure of reactant A at the reaction surface, and k and K are the constants in the Langmuir–Hinshelwood rate expression.

Many gas–solid reactions, especially those involving metal compounds, obey this rate law. It can be shown, furthermore, that by the appropriate transformation [11] the results obtained for rate expressions of the type given by Eq. (1) may be valid for the description of systems obeying more complex rate laws, e.g.

$$R_A = \frac{k(P_A - P_x/K_{eq})}{1+K_AP_A+\sum_i K_iP_i+\sum_j K_{Ij}P_{Ij}} \tag{2}$$

This rate expression takes into account a reversible chemical reaction on the solid surface and the adsorption of species that participate in the reaction as well as the adsorption of inert species.

Within a narrow range of pressure Eq. (1) may be approximated by the following relationship:

$$R_A \alpha P_A^{1/n}; (n > 1) \tag{3}$$

which has been used frequently to describe the pressure dependence of the rate of a gas–solid reaction.

It is noted, however, that in the reaction of porous solids the diffusional resistance may lead to the existence of a gradient in the partial pressure of the reactant gas—within the pellet. Under these conditions the apparent "reaction order" may change from a low value at the outside surface to a value approaching unity in the interior of the pellet. This behavior is the major disadvantage of Eq. (3) for the interpretation of experimental data when both diffusional and kinetic effects are important.

FORMULATION

Let us consider a porous solid, made up of individual grains. Both the macroscopic solid pellet and the grains may have the shape of a sphere, a cylinder or an infinite slab. Let this solid pellet undergo an irreversible chemical reaction with a reactant gas, according to the rate expression given by Eq. (1). The formulation of this problem for first-order surface kinetics and isothermal conditions has been given in the previous paper. By using an analogous procedure described in Ref.[1] the governing equations may be put in the following dimensionless forms:

The conversation of the gaseous reactant may be written as

$$\nabla^{*2} \psi - 2F_g F_p \hat{\sigma}^2 \xi^{F_g - 1} \frac{(1+\kappa)\psi}{1+\kappa\psi} = 0 \tag{4}$$

and a mass balance on the solid grains is given as

$$\frac{\partial \xi}{\partial t^*} = -\frac{(1+\kappa)\psi}{1+\kappa\psi} \tag{5}$$

where

$$\hat{\sigma} \equiv \frac{V_p}{A_p} \sqrt{\frac{(1-\epsilon)F_p}{2D_e}\left(\frac{k}{1+\kappa}\right)\left(\frac{A_g}{F_g V_g}\right)} \tag{6}$$

$$\kappa \equiv KP_{AS} \tag{7}$$

and

$$t^* \equiv \frac{bkP_{AS}}{\rho_m(1+\kappa)}\left(\frac{A_g}{F_g V_g}\right) t \tag{8}$$

The other variables and parameters are defined in the notation. In the absence of external-mas-transfer resistance, the initial and boundary conditions are

$$\xi = 1 \quad \text{at } t^* = 0 \tag{9}$$

$$\psi = 1 \quad \text{at } \eta = 1 \tag{10}$$

$$\frac{\partial \psi}{\partial \eta} = 0 \quad \text{at } \eta = 0. \tag{11}$$

The solution of Eqs. (4) and (5) will yield ξ as a function of η and t^*. The overall conversion can then be calculated from the following relationship:

$$X = \frac{\int_0^1 \eta_p^{(F-1)}(1-\xi_g^F)\,d\eta}{\int_0^1 \eta_p^{(F-1)}\,d\eta}. \tag{12}$$

The forms of the above dimensionless variables were chosen such that, as κ becomes ∞, the equations reduce directly to those for a zeroth-order reaction. When κ is zero, the governing equations reduce to those previously given for a first-order reaction.

The generalized gas–solid reaction modulus, $\hat{\sigma}$, which is defined by taking into consideration the shapes of both the pellet and the individual grains, has been proved quite useful[1] in presenting and generalizing the conversion vs. time relationship for various geometries. The parameter $\hat{\sigma}$ also provided a convenient criterion for the assessment of the relative importance of chemical and diffusion control—without regard to geometry. As will be shown subsequently, through the definition of $\hat{\sigma}$ in Eq. (6) similar considerations will apply to Langmuir–Hinshelwood kinetics.

It was also shown in the previous paper[1] that, for first-order kinetics, the relationship

between the conversion and the reaction time for various pellet and grain geometries can be expressed by the following approximate, but very simple expression:

$$t^* = g_{F_g}(X) + \hat{\sigma}^2 p_{F_p}(X) \tag{13}$$

where

$$g_{F_g}(X) \equiv 1-(1-X)^{1/F_g} \tag{14}$$

and

$$p_{F_p}(X) \equiv$$

$$\begin{cases} X^2 & \text{for } F_p = 1 \quad (15) \\ X+(1-X)\ln(1-X) & \text{for } F_p = 2 \quad (16) \\ 1-3(1-X)^{2/3}+2(1-X) & \text{for } F_p = 3. \quad (17) \end{cases}$$

It could be expected that the equivalent form of Eq. (13) will become less satisfactory as the reaction order departs from unity. It will be shown, however, that Eq. (9) holds approximately for a Langmuir–Hinshelwood type of kinetics provided $\kappa < 1$ and $\hat{\sigma}$ and t^* are defined as in Eqs. (6) and (8), respectively.

RESULTS

In general, Eqs. (4) and (5) have to be solved numerically. Before presenting a general set of solutions it may be worthwhile to examine the asymptotic behavior of the system, for small and large values of $\hat{\sigma}$, which correspond to chemical and product-layer diffusion control, respectively.

1. *Asymptotic behavior*

i. *Chemical reaction control.* When the rate of the chemical reaction is much slower than that of diffusion within the pellet, i.e. $\hat{\sigma} \to 0$, the reactant concentration is uniform throughout the pellet and equal to that at the external surface ($\psi = 1$). Under these conditions Eq. (5) is readily integrated to give

$$\xi = \begin{cases} 1-t^* & \text{for } 0 \leq t^* \leq 1 \\ 0 & \text{for } 1 \leq t^*. \end{cases} \tag{18}$$

The relationship between the conversion and the reaction time is then found, by combining Eqs. (12) and (18) to obtain

$$t^* = g_{F_g}(X). \tag{19}$$

This relationship, which is identical to that previously given for first-order kinetics[1], holds regardless of the value of κ in the Langmuir–Hinshelwood expression.

Information on F_g and on the intrinsic reaction parameters can then be readily obtained within this region by using Eq. (19), as described in Ref. [1].

ii. *Product-layer diffusion control.* When the rate of the chemical reaction is much faster than that of diffusion, i.e. $\hat{\sigma} \to \infty$, the concentration of the gaseous reactant becomes zero at the interface between the completely reacted and the unreacted zones. The reaction kinetics are not rate limiting, and the relationship between the conversion and the reaction time is given by

$$t^*/\hat{\sigma}^2 = p_{F_p}(X). \tag{20}$$

The effective diffusivity in the product layer can then be determined from experimental data using Eq. (20) under conditions where $\hat{\sigma}$ is large.

2. *Analytic solutions – special cases*

If κ approaches infinity (zeroth-order reaction) in a system with $F_g = 1$, analytic solution is possible. Under these conditions, the second term (the local rate of reaction) becomes constant and $\partial\xi/\partial t^* = 1$. The concentration of the gaseous reactant becomes zero at a certain point η_1 within the pellet, if $\hat{\sigma}$ is sufficiently large ($\hat{\sigma} > 1$ as will be shown below). This reactant exhaustion phenomenon is unique for a zeroth-order reaction and is a consequence of the rate being independent of concentration. This position η_1 remains fixed until all the solid at $\eta \geq \eta_1$ is completely reacted. The duration of this period is obtained from Eq. (5) as $t_1^* = 1$. In the next stage the contration becomes zero at a point further inside, η_2. At $\eta > \eta_1$ only diffusion occurs, and the concentration and its gradient must be matched at $\eta = \eta_1$. After $t_2^* = t_1^* + 1$ the

layer at $\eta_2 < \eta < \eta_1$ is completely reacted. This process is continued until the concentration at the center of the pellet is no longer zero and the grains at $\eta = 0$ are completely reacted. The solution thus obtained for pellets of various shapes takes the following form:

When $m-1 \leq \sigma \leq m$, (m is an integer)

$$X = 1 - \eta_i^{F_p} - (\eta_{i-1}^{F_p} - \eta_i^{F_p})(i - t^*)$$

$$\text{for } i-1 \leq t^* \leq i; \quad i = 1, 2, \ldots, m-1$$

and

$$X = 1 - (m - t^*)\eta_{m-1}^{F_p}$$

$$\text{for } m-1 \leq t^* \leq m \qquad (21)$$

where

$$p_{F_p}(1 - \eta_i^{F_p}) = i/\hat{\sigma}^2.$$

The function $p_{F_p}(x)$ has been defined by Eqs. (15)–(17).

It should be noted at this stage that the zeroth-order reaction corresponds to an asymptotic behavior which may not be readily realized in gas–solid reaction systems. It follows that the expressions developed here for zeroth-order behavior represent a limiting case which may not be readily attained by practical systems.

3. *The general case*

In general Eqs. (4) and (5) must be solved numerically. Equation (4), which is nonlinear, was solved using the technique of linearization about a trial solution and subsequent iteration, as described by Newman[12].

Figures 1(a) and (b) show the effect of κ on the relationship between the conversion and time for different values of $\hat{\sigma}$. The geometries considered are a slab-like pellet made up of flat grains ($F_g = F_p = 1$) and a spherical pellet made up of spherical grains ($F_g = F_p = 3$). These two systems are considered to represent the two extremes of the nine possible combinations.

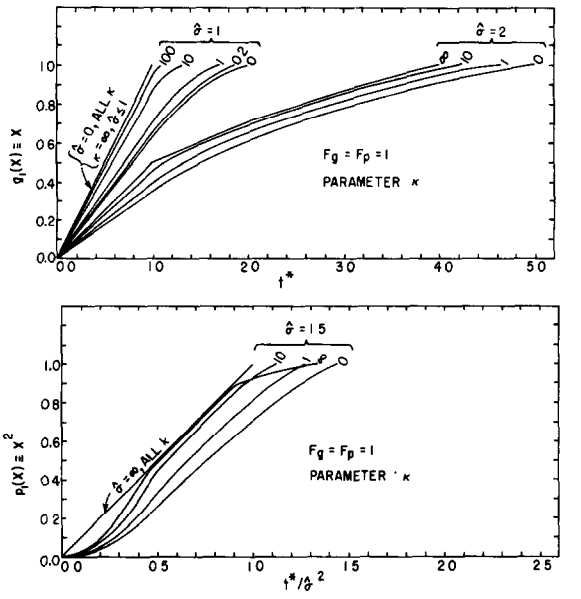

Fig. 1(a).

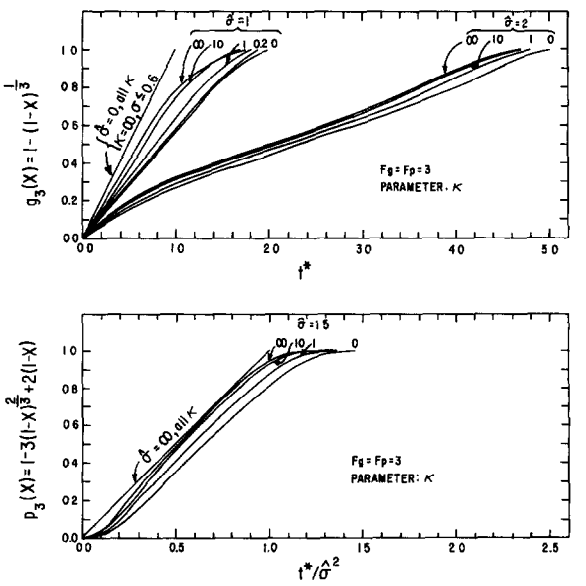

Fig. 1(b).

Fig. 1. Effect of κ on conversion vs. time relationship for different values of $\hat{\sigma}$. (a) $F_g = F_p = 1$, (b) $F_g = F_p = 3$.

It is seen that for the same reaction rate at the bulk conditions (see the definition of t^*), it takes generally less time to achieve a certain conversion as the value of κ increases. Physically, this is because the rate becomes less dependent on concentration as κ increases. When κ is very

large, the time required for a high conversion may become larger than that for a smaller κ. (See Fig. 4 below.)

The effect of κ is largest for $\hat{\sigma}$ around unity, i.e. when chemical reaction and diffusion are of comparable importance. When $\hat{\sigma}$ approaches zero, Eq. (19) holds and is valid for all values of κ. On the other hand, when $\hat{\sigma}$ approaches ∞, Eq. (20) becomes the solution regardless of the reaction kinetics.

The curves for $F_g = F_p = 1$ and $F_g = F_p = 3$ with the same value of $\hat{\sigma}$ are very similar to each other, when $g_{F_g}(X)$ is plotted against t^* for small $\hat{\sigma}$ and $p_{F_p}(X)$ against $t^*/\hat{\sigma}^2$ for large σ as in these figures. This is one of the convenient features of using $g(X)$ and $p(X)$ functions as well as the "generalized as-solid reaction modulus" $\hat{\sigma}$.

It is noted that, as κ increases, the curve approaches that for $\hat{\sigma} = 0$ when $\hat{\sigma}$ is smaller than a certain value depending on system geometries. When $\hat{\sigma}$ is large (say $\hat{\sigma} > 2$), the curve approaches that for $\hat{\sigma} \to \infty$ as κ increases.

The curves for $\hat{\sigma} = 1$ show that, as far as the conversion vs. time relationship is concerned, first-order kinetics ($\kappa = 0$) may be assumed for $\kappa > 0{\cdot}2$ and zeroth-order kinetics ($\kappa = \infty$) may be assumed for $\kappa > 100$.

Figures 2–4 show the effect of κ on the time required to reach 30, 60 and 100 per cent conversion as a function of $\hat{\sigma}$. The ordinate may be regarded as an overall effectiveness factor up to that conversion value chosen in each figure. The abscissa was chosen such that the large $\hat{\sigma}$ asymptote may be brought to the same position for different conversions. Such coordinates were first used in Ref. [1].

It is noted that the broken line appearing on the right hand side denotes the diffusion limited asymptote.

Inspection of Figs. 2–4 shows that in general the solutions are bounded between the asymptotes corresponding to $\kappa = 0$ and $\kappa = \infty$. The only exception to this rule is the behavior found for high values of conversion and for very high values of κ, particularly notable in Figs. 1 and 4a. It is quite likely, however that the shape

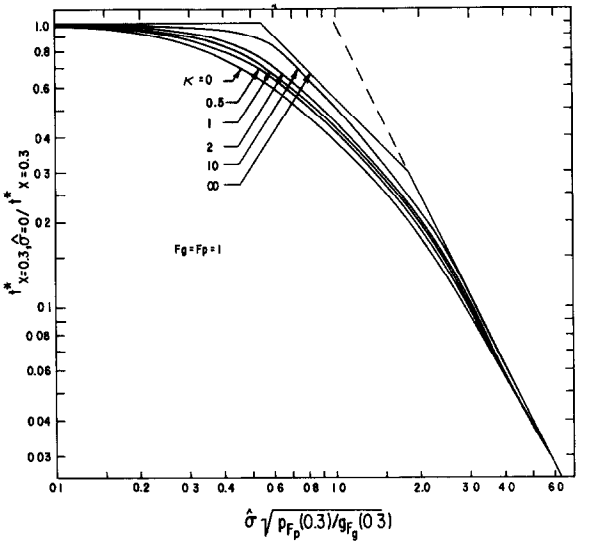

Fig. 2(a).

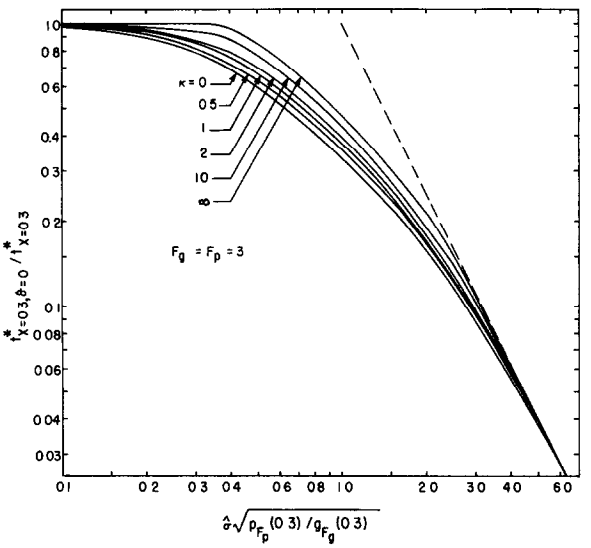

Fig. 2(b).

Fig. 2. Effect of κ on time vs. $\hat{\sigma}$ relationship for 30 per cent conversion. (a) $F_g = F_p = 1$, (b) $F_g = F_p = 3$.

of the $\kappa \to \infty$ asymptote in Fig. 4a owes its existence to the mathematical formalism for zeroth-order reaction, rather than being a consequence of physical reality.

Although the solution depends on the value of κ, the curves for $\kappa < 1$ lie close to those for $\kappa = 0$ (first-order kinetics) for which Eq. (13)

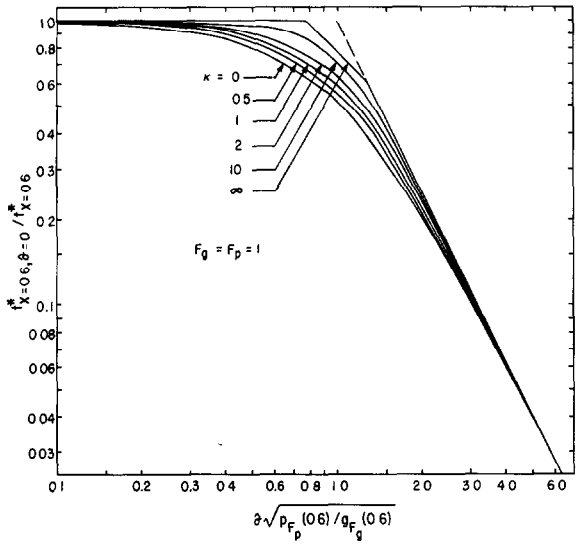

Fig. 3(a).

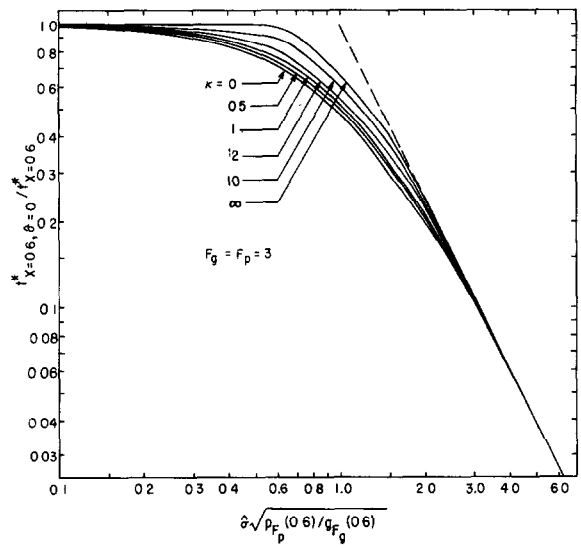

Fig. 3(b).

Fig. 3. Effect of κ on time vs. $\hat{\sigma}$ relationship for 60 per cent conversion. (a) $F_g = F_p = 1$, (b) $F_g = F_p = 3$.

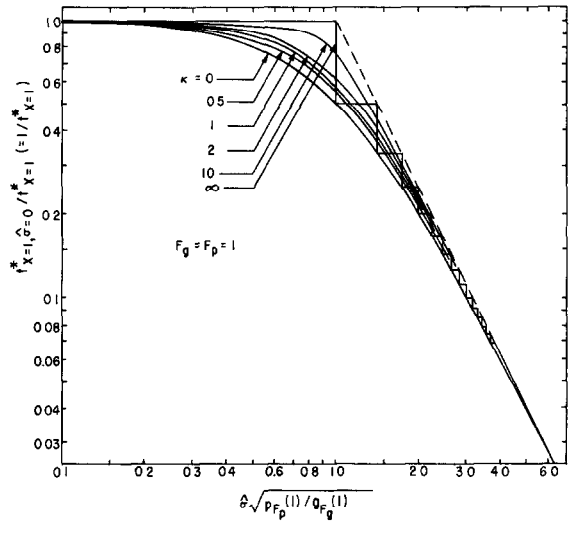

Fig. 4(a).

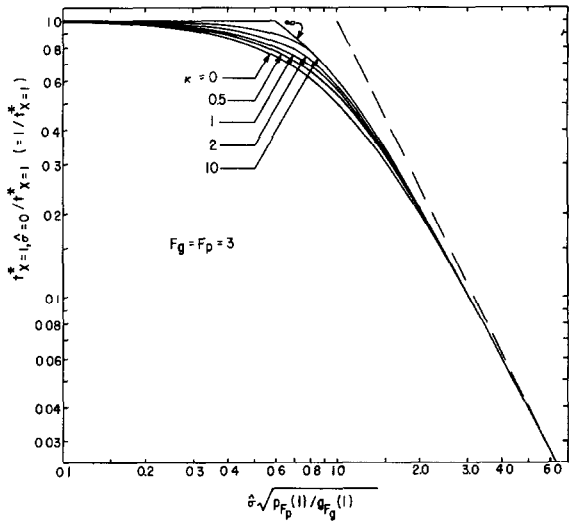

Fig. 4(b).

Fig. 4. Effect of κ on time vs. $\hat{\sigma}$ relationship for complete conversion. (a) $F_g = F_p = 1$, (b) $F_g = F_p = 3$.

holds approximately. Figure 5 shows explicitly the comparison between Eq. (13) and the exact solutions for different values of κ. It can be said that Eq. (13) approximates the exact solution for $\kappa < 1$. The comparison is made for $\hat{\sigma} = 1$ for which the effect of κ is largest. For smaller and larger values of $\hat{\sigma}$ the agreement is better than shown in this figure, Eq. (13) becoming asymptotically correct as $\hat{\sigma} \to 0$ or ∞ regardless of the value of κ.

Figures 6 (a) and (b) show the rate of conversion at different extents of conversion. The ordinate may be considered as the average rate

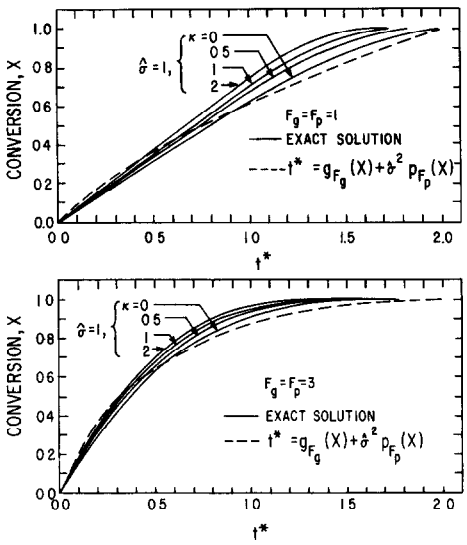

Fig. 5. Comparison of Eq. (13) with exact solution for different values of κ.

of penetration of the reaction interface within the individual grains. Here again, the effect of κ is seen to be greatest when $\hat{\sigma}$ is about unity. The rate is in general higher for larger values of κ at the same conversion.

It is noted that, for both geometries considered, the diffusional resistance may be neglected if $\hat{\sigma} < 0{\cdot}3$. The rate, $dg_{F_g}(X)/dt^*$ is close to unity during almost the entire duration of reaction, regardless of the value of κ. On the other hand, when $\hat{\sigma} > 3$ the overall rate is controlled by the diffusion in the product layer, and κ has little effect on the rate except during the initial and the final stages of the reaction. It may be worthwhile to note the rather peculiar shape of the curves, corresponding to $\kappa = \infty$. It is thought, however, that no particular physical significance should be attached to this.

When the amount of the solid that is completely converted is of interest, the thickness of the completely reacted layer rather than the overall conversion is important. Figures 7 (a) and (b) show the position of the interface between the completely reacted layer and the partially reacted core, as a function of time, for various value of $\hat{\sigma}$ and κ. It is seen that in all the cases the interface is not established until $t^* = 1$, i.e. until the

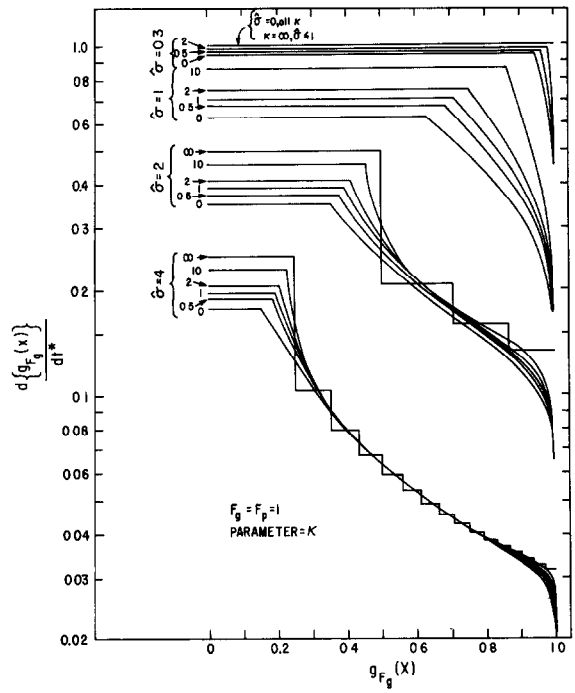

Fig. 6(a).

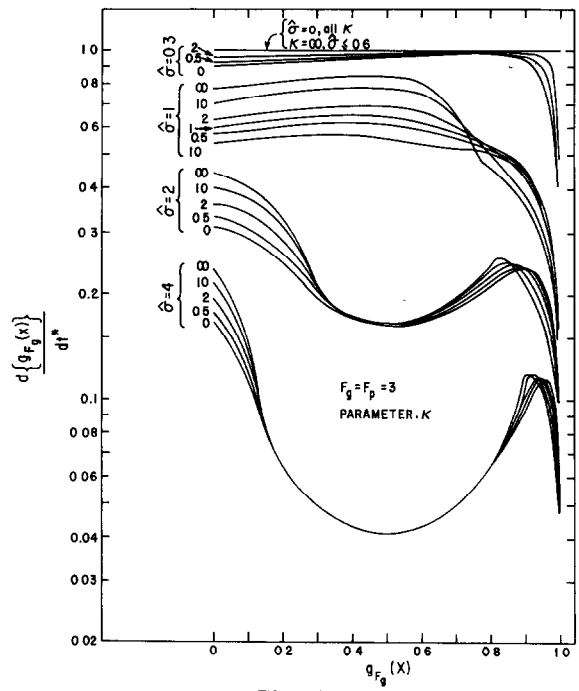

Fig. 6(b).

Fig. 6. Effect of κ on the rate of conversion for different values of $\hat{\sigma}$. (a) $F_g = F_p = 1$, (b) $F_g = F_p = 3$.

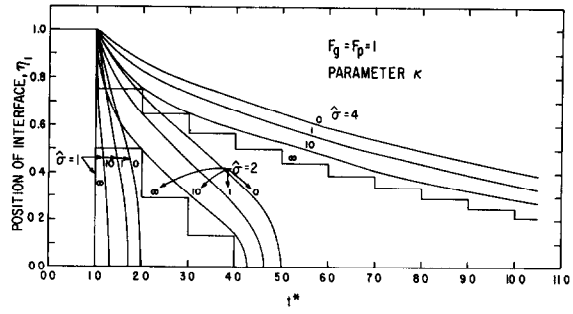

Fig. 7(a).

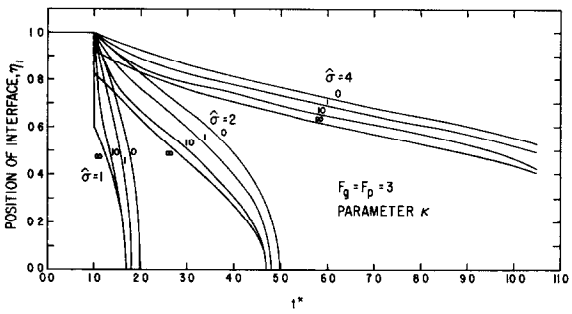

Fig. 7(b).

Fig. 7. Effect of κ on the position of interface between the completely reacted layer and the partially reacted core. (a) $F_g = F_p = 1$. (b) $F_g = F_p = 3$.

attainment of the time required to react the outermost layer of the pellet completely. As $\hat{\sigma}$ increases, the rate of penetration of the interface becomes slower as one may on physical grounds expect. For the same value of $\hat{\sigma}$, the rate of penetration is faster for a larger κ. This behavior is due to the fact that the concentration dependence of the rate decreases as κ increases. It follows that for decreasing reactant concentration within the pellet, the reaction rate falls at a lower rate for larger values of κ.

CONCLUSIONS

1. The value of κ in the Langmuir–Hinshelwood type of kinetic expressions influences the relationship between the conversion and the reaction time in the reaction of a porous solid with a gas. The effect is largest in the region where chemical reaction and diffusion are of comparable importance ($\hat{\sigma} \approx 1$). In the regimes controlled either by chemical reaction or by diffusion in the product layer, the effect of κ is negligible.

2. The numerical values of $\hat{\sigma}$ that characterize the regions of different control remain the same regardless of the value of κ and of the geometries of the system, provided that $\hat{\sigma}$ is defined as in Eq. (6). Thus, a system with $\hat{\sigma} < 0{\cdot}3$ is controlled by chemical reaction and under these conditions the whole pellet reacts uniformly throughout. When $\hat{\sigma} > 3$, the overall rate is controlled by diffusion in the product layer, and the reaction occurs along a sharp interface within the pellet between the completely reacted layer and the completely unreacted core. In the intermediate regime, the overall rate is determined by both chemical reaction and diffusion, and the reaction occurs in a diffuse zone.

3. A first-order behavior ($\kappa = 0$) is approached when $\kappa < 0{\cdot}2$ and a zeroth-order behavior ($\kappa = \infty$) is approached when $\kappa > 100$. This information is useful in that the analysis for a first-order or a zeroth-order kinetics is much simpler than that for Langmuir–Hinshelwood type of kinetics which gives rise to a non-linear term in the mass balance equation.

4. The approximate equation for the conversion vs. time relationship (Eq. 13), which was obtained for first-order kinetics, may be used for a system with κ up to about unity without introducing too great an error.

5. The solutions obtained are also applicable, with proper transformation of variables, to a more general rate expression (Eq. 2) which takes into account a reversible chemical reaction on the solid surface and the adsorption of all the species present in the system.

Acknowledgements—The authors wish to thank Professor Y. K. Rao of Columbia University for drawing attention to the problem, and thanks are also due to the A. E. Anderson Foundation for partial support of this investigation through a grant to the Center for Process Metallurgy.

NOTATION

A_g, A_p external surface area of an individual grain and the pellet, respectively

b number of moles of the solid reacted per unit mole of the gaseous reactant

D_e effective diffusivity of the gaseous reactant within the pellet

F_g, F_p shape factor for the grains and the pellet, respectively (= 1, 2 and 3 for infinite slabs, long cylinders, and spheres, respectively)

$g(X)$ conversion function defined by Eq. (14)

k, K parameters in Langmuir–Hinshelwood expression (Eq. 1)

$p(X)$ conversion function defined by Eqs. (15)–(17)

P_A, P_{AS} partial pressure of the gaseous reactant within the pellet and at the external surface of the pellet, respectively

r postion of the moving reaction front in the individual grain

R distance coordinate in the pellet

t time

t^* dimensionless time defined by Eq. (8)

V_g, V_p volume of an individual grain and the pellet, respectively

X fractional conversion of solid reactant

Greek symbols

ϵ porosity of the pellet

η dimensionless distance coortinate ($\equiv A_p R/F_p V_p$)

κ dimensionless parameter defined by Eq. (7)

ξ dimensionless position of the reaction front in the grain ($\equiv A_g r/F_g V_g$)

ρ_m molar density of the solid

$\hat{\sigma}$ generalized gas–solid reaction modulus defined by Eq. (6)

ψ dimensionless partial pressure of the gaseous reactant ($\equiv P_A/P_{AS}$)

Other symbols

∇^{*2} Laplacian operator with η as the position coordinate

REFERENCES

[1] SOHN H. Y. and SZEKELY J., *Chem. Engng Sci.* 1972 **27** 763.
[2] QUETS J. M., WADSWORTH M. E. and LEWIS J. R., *Trans. Metall. Soc. A.I.M.E.* 1961 **221** 1186.
[3] McKEWAN W. M., *Trans. Metall. Soc. A.I.M.E.* 1962 **224** 387.
[4] KUROSAWA T., HASEGAWA R. and YAGIHASHI T., *Nippon Kinzoku Gakkaishi* 1970 **34** 481.
[5] MOREAU C. and PHILIPPOT J., *Proc. 6th Int. Symp. on the Reactivity of Solids*, p. 377 1969.
[6] WALKER P. L., JR., RUSINKO F., JR. and AUSTIN L. G., *Adv. Catal.* 1959 **XI** 133.
[7] DELMON B., *Introduction a la Cinétique Hétérogène*, Chapt. 3, Éditions Technip, Paris 1969.
[8] ROZOVSKII A. YA. and SHCHEKIN V. V., *Kinet. Katal.* 1960 **1** 313; *Kinet. Catal.* 1960 **1** 286.
[9] CHU C. and HOUGEN O. A., *Chem. Engng Sci.* 1962 **17** 167.
[10] ROBERTS G. W. and SATTERFIELD C. N., *Ind. Engng Chem. Fundls* 1965 **4** 288; 1966 **5** 317.
[11] SCHNEIDER P. and MITSCHKA P., *Chem. Engng Sci.* 1966 **21** 455.
[12] NEWMAN J., *Ind. Engng Chem. Fundls* 1968 **7** 514.